



# A qualitative comparison of secondary organic aerosol yields and composition from ozonolysis of monoterpenes at varying concentrations of NO<sub>2</sub>

D. C. Draper<sup>1,a</sup>, D. K. Farmer<sup>2</sup>, Y. Desyaterik<sup>3</sup>, and J. L. Fry<sup>1</sup>

<sup>1</sup>Department of Chemistry, Reed College, Portland, OR, USA

<sup>2</sup>Department of Chemistry, Colorado State University, Fort Collins, CO, USA

<sup>3</sup>Department of Atmospheric Science, Colorado State University, Fort Collins, CO, USA

<sup>a</sup>current address: Department of Chemistry, University of California Irvine, Irvine, CA, USA

Correspondence to: J. L. Fry (fry@reed.edu)

Received: 25 April 2015 – Published in Atmos. Chem. Phys. Discuss.: 28 May 2015

Revised: 30 September 2015 – Accepted: 25 October 2015 – Published: 5 November 2015

**Abstract.** The effect of NO<sub>2</sub> on secondary organic aerosol (SOA) formation from ozonolysis of  $\alpha$ -pinene,  $\beta$ -pinene,  $\Delta^3$ -carene, and limonene was investigated using a dark flow-through reaction chamber. SOA mass yields were calculated for each monoterpene from ozonolysis with varying NO<sub>2</sub> concentrations. Kinetics modeling of the first-generation gas-phase chemistry suggests that differences in observed aerosol yields for different NO<sub>2</sub> concentrations are consistent with NO<sub>3</sub> formation and subsequent competition between O<sub>3</sub> and NO<sub>3</sub> to oxidize each monoterpene.  $\alpha$ -Pinene was the only monoterpene studied that showed a systematic decrease in both aerosol number concentration and mass concentration with increasing [NO<sub>2</sub>].  $\beta$ -Pinene and  $\Delta^3$ -carene produced fewer particles at higher [NO<sub>2</sub>], but both retained moderate mass yields. Limonene exhibited both higher number concentrations and greater mass concentrations at higher [NO<sub>2</sub>]. SOA from each experiment was collected and analyzed by HPLC-ESI-MS, enabling comparisons between product distributions for each system. In general, the systems influenced by NO<sub>3</sub> oxidation contained more high molecular weight products (MW > 400 amu), suggesting the importance of oligomerization mechanisms in NO<sub>3</sub>-initiated SOA formation.  $\alpha$ -Pinene, which showed anomalously low aerosol mass yields in the presence of NO<sub>2</sub>, showed no increase in these oligomer peaks, suggesting that lack of oligomer formation is a likely cause of  $\alpha$ -pinene's near 0 % yields with NO<sub>3</sub>. Through direct comparisons of mixed-oxidant systems, this work suggests that NO<sub>3</sub> is likely to dominate nighttime oxidation pathways in most regions with both biogenic and

anthropogenic influences. Therefore, accurately constraining SOA yields from NO<sub>3</sub> oxidation, which vary substantially with the volatile organic compound precursor, is essential in predicting nighttime aerosol production.

## 1 Introduction

Secondary organic aerosol (SOA) forms in the atmosphere from oxidized volatile organic compounds (VOCs) that are of low enough volatility to be able to partition into the condensed phase. Aerosol directly affects Earth's radiative balance and also contributes to cloud formation, both of which have important climate forcing implications (IPCC, 2013). Aerosol is responsible for regional haze and has been shown to cause adverse cardiopulmonary health effects (Pope III et al., 1995; Davidson et al., 2005). SOA constitutes a large fraction of the total aerosol budget, but it is still poorly constrained in global chemical transport models, which underpredict ambient aerosol concentrations by 1 to 2 orders of magnitude (Heald et al., 2005, 2011). These models use laboratory-derived parameters, but uncertainty in precursors, detailed mechanisms, and mechanistic differences between chamber simulations and the real atmosphere result in the vast discrepancies between models and observations (Kroll and Seinfeld, 2008; Hallquist et al., 2009).

Nearly 90 % of the non-methane VOCs emitted globally are biogenic in origin, so it should follow that a large frac-

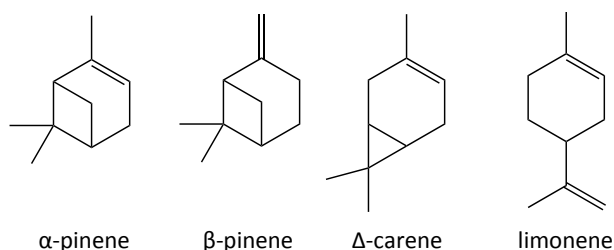


**Figure 1.** Structures of monoterpenes used in this study.

tion of the uncertainty in model predictions of the SOA budget comes from uncertainty in how biogenic VOCs (BVOCs) form aerosol (Guenther et al., 1995; Middleton, 1995). Different plant species emit different types and ratios of BVOCs, so the specific distribution of BVOCs emitted to the atmosphere is dependent on unique mixtures of vegetation and thus varies a great deal regionally. Monoterpenes are one such class of BVOC that is both widely emitted and has been shown in the laboratory to efficiently produce SOA (Goldstein and Galbally, 2007; Sakulyanontvittaya et al., 2008; Griffin et al., 1999; Hallquist et al., 1999; Ng et al., 2006; Ehn et al., 2014; Hoyle et al., 2011). On average in the United States,  $\alpha$ -pinene is the most dominant monoterpene emission, but  $\beta$ -pinene,  $\Delta^3$ -carene, and limonene (Fig. 1) are also prevalent and are emitted equally or more than  $\alpha$ -pinene in some regions (Geron et al., 2000).

While most VOCs are biogenic, the majority of atmospheric oxidants are anthropogenically sourced, and thus human activity is highly influential on SOA production (Carlton et al., 2010; Hoyle et al., 2011; Xu et al., 2015). At night, most VOC oxidation in the troposphere occurs by way of either photolabile nitrate radical (NO<sub>3</sub>) or longer-lived ozone (O<sub>3</sub>), which is photochemically produced but is not rapidly and completely consumed at sundown as is the hydroxyl radical (OH). The formation of both of these tropospheric oxidants requires NO<sub>2</sub>, nearly 90 % of which in the USA (64 % globally) is estimated to come from anthropogenic sources (Reis et al., 2009). Organonitrates have been observed in ambient nighttime aerosol during multiple field studies (Fry et al., 2013; Rollins et al., 2012; Xu et al., 2015), consistent with NO<sub>3</sub> oxidation, and NO<sub>3</sub> initiated production of aerosol organonitrates may even compete with photolysis of NO<sub>3</sub> during the day in some regions with high BVOC emissions (Ayres et al., 2015). These observations are consistent with several laboratory studies that have found moderate to high aerosol yields from NO<sub>3</sub> oxidation (Griffin et al., 1999; Hallquist et al., 1999; Fry et al., 2009, 2011, 2014; Spittler et al., 2006; Moldanova and Ljungström, 2000; Boyd et al., 2015), but this body of literature is comparatively small relative to OH and O<sub>3</sub> oxidation studies.

Most chamber studies of NO<sub>3</sub>-derived SOA generate NO<sub>3</sub> through the thermal dissociation of N<sub>2</sub>O<sub>5</sub> in order to minimize the complexity caused by introducing a second ox-

dant (Griffin et al., 1999; Hallquist et al., 1999; Fry et al., 2014). Fewer studies have been done using the atmospherically more relevant conditions of introducing both O<sub>3</sub> and NO<sub>2</sub> into the chamber to mimic this full range of nighttime oxidation chemistry (Perraud et al., 2012; Presto et al., 2005; Boyd et al., 2015). Perraud et al. (2012) and Presto et al. (2005) both studied the effects of a range of NO<sub>2</sub> concentrations on dark ozonolysis of  $\alpha$ -pinene, and both observed that increased [NO<sub>2</sub>] suppresses aerosol formation. To our knowledge, NO<sub>2</sub> effects on dark ozonolysis have not been systematically assessed for any other monoterpenes. Ozonolysis of  $\alpha$ -pinene has been previously observed to have high (14–67 %) aerosol yields (Hoffmann et al., 1997; Ng et al., 2006) but strikingly low (0–16 %) SOA yields with NO<sub>3</sub> (Hallquist et al., 1999; Fry et al., 2014; Spittler et al., 2006). The observed aerosol suppression in the O<sub>3</sub> + NO<sub>2</sub> system is consistent with the increased contribution of NO<sub>3</sub> at higher [NO<sub>2</sub>]. However,  $\alpha$ -pinene is the only monoterpene that has been observed to have such drastic SOA yield discrepancies between the two oxidants (Ng et al., 2006; Yu et al., 1999; Hallquist et al., 1999; Fry et al., 2014), so it may not be reasonable to assume NO<sub>2</sub> has the same effect on other monoterpenes.

Here we focus on the four most prevalently emitted monoterpenes in the US:  $\alpha$ -pinene,  $\beta$ -pinene,  $\Delta^3$ -carene, and limonene. Table 1 shows rate constants for NO<sub>3</sub> formation from NO<sub>2</sub> + O<sub>3</sub> as well as each of the nighttime oxidants with the monoterpenes used in this study. It is evident that the rates of O<sub>3</sub> loss to NO<sub>3</sub> production and BVOC oxidation are comparable when [NO<sub>2</sub>] and [BVOC] are similar. Even considering its smaller ambient concentrations, NO<sub>3</sub> oxidation is often much faster than O<sub>3</sub> oxidation, so it follows that NO<sub>3</sub> oxidation should provide an important contribution to nighttime aerosol formation in regions that are both biogenically and anthropogenically influenced. This work seeks to characterize the role of each competing nighttime oxidant over this broader range of monoterpenes and the influence of each on SOA formation.

## 2 Methods

Unseeded SOA formation experiments were performed in a darkened  $\sim$ 400 L PFA film chamber, shown in Fig. 2, run in flow-through mode with precursors added continuously, giving a residence time of approximately 90 min. The set of experiments described in Table 2 measured the aerosol production from a single monoterpene oxidized by O<sub>3</sub> with varying concentrations of NO<sub>2</sub> added. In order to make comparisons across both the range of monoterpenes and the range of [NO<sub>2</sub>], the monoterpene source and O<sub>3</sub> source concentrations were kept as constant as possible throughout the full study, allowing only the identity of the BVOC and the concentration of NO<sub>2</sub> to vary. While precursor concentrations used in this study are all quite high and thus absolute ob-

**Table 1.** Rate constants at 298 K for NO<sub>2</sub> + O<sub>3</sub> (Sander et al., 2011) and for both O<sub>3</sub> and NO<sub>3</sub> with selected monoterpenes (Atkinson and Arey, 2003).

	$k \times 10^{17}$ (cm <sup>3</sup> molec <sup>-1</sup> s <sup>-1</sup> )	$k_{\text{O}_3} \times 10^{17}$ (cm <sup>3</sup> molec <sup>-1</sup> s <sup>-1</sup> )	$k_{\text{NO}_3} \times 10^{12}$ (cm <sup>3</sup> molec <sup>-1</sup> s <sup>-1</sup> )
NO <sub>2</sub> + O <sub>3</sub>	3.2	–	–
$\alpha$ -Pinene	–	8.4	6.2
$\beta$ -Pinene	–	1.5	2.51
$\Delta^3$ -Carene	–	3.7	9.1
Limonene	–	21	12.2

served aerosol yields are likely not atmospherically relevant due to high-mass loadings and unrealistic radical fates, the ratios of [O<sub>3</sub>] : [NO<sub>2</sub>] ranging from 1 : 0.5 to 1 : 4 are representative of ratios observable in the atmosphere from relatively clean sites (O<sub>3</sub> dominated) to heavily polluted sites (NO<sub>2</sub> dominated). Similarly, [NO<sub>2</sub>] : [BVOC] ranging from approximately 1 : 1 to 2 : 1 is reasonable for relatively clean to relatively polluted sites, making comparisons between these conditions informative to aerosol formation in the real atmosphere.

O<sub>3</sub> (and NO<sub>2</sub>, when applicable) were introduced into the chamber first and allowed to reach steady state prior to initiation of SOA formation by BVOC injection. O<sub>3</sub> was generated by flowing zero air (Sabio Model 1001 compressed zero air generator) through a flask containing a Pen-Ray Hg lamp (primary energy at 254 nm) and was continuously measured from the outlet of the chamber using a Dasibi Model 1003-AH O<sub>3</sub> monitor. NO<sub>2</sub> was introduced from a calibrated cylinder (Air Liquide, 0.3 % by volume in N<sub>2</sub>) and monitored using a Thermo Model 17i chemiluminescence NO<sub>x</sub>/NH<sub>3</sub> analyzer. Chemiluminescence NO<sub>x</sub> analyzers are sensitive to any species that is converted to NO in the 350 °C Mb converter responsible for converting NO<sub>2</sub> to NO (Winer et al., 1974; Grosjean and Harrison, 1985). Some of these additional species include N<sub>2</sub>O<sub>5</sub>, peroxy nitrates (PNs), and alkyl nitrates (ANs). At the high concentrations used in this study, these NO<sub>y</sub> contributions were significant. Kinetics modeling of the oxidant stabilization period (described in the Supplement), corroborated by a characterization of oxidant stabilization using chemiluminescence NO<sub>x</sub> analyzers and a cavity ring-down spectrometer sensitive only to NO<sub>2</sub>, indicates that we detected N<sub>2</sub>O<sub>5</sub> with approximately unit efficiency in the NO<sub>2</sub> channel of the Thermo NO<sub>x</sub> analyzer. The sensitivity of this NO<sub>x</sub> analyzer to PNs and ANs, which would have formed following BVOC addition, was not calibrated, but is expected to be near unity based on previous studies (Winer et al., 1974; Grosjean and Harrison, 1985). Modeling only the oxidant stabilization period, where NO<sub>2</sub> and N<sub>2</sub>O<sub>5</sub> were likely the only species detected in the NO<sub>2</sub> channel, provided the initial NO<sub>2</sub> concentrations shown in Table 2.

Once the oxidants stabilized, BVOC was introduced by flowing zero air over a small, cooled liquid sample of the tar-

get BVOC ((1R)-(+)-alpha-Pinene, TCI America, > 95.0 %; (–)-beta-Pinene, TCI America, > 94 %; (+)-3-Carene, TCI America, > 90.0 %; (R)-(+)-Limonene, Aldrich, > 97 %). The chiller temperature was held constant ( $\pm 0.3$  °C) during a single experiment and ranged from –27 to –21 °C for the different monoterpenes, based on the temperature-dependent vapor pressure that is calculated to give a mixing ratio of approximately 100 ppm in the source flask (Fig. S3 in the Supplement) (Haynes et al., 2012). Since vapor pressure data were unavailable for  $\Delta^3$ -carene, it was estimated to reach the temperature-dependent vapor pressure at –25 °C – between  $\alpha$ -pinene and  $\beta$ -pinene's target temperatures – due to structural similarities. Online BVOC measurements were not available, but reacted BVOC was calculated from the observed decay of the oxidant in the kinetics model for each experiment. Methodology and uncertainties of this approach are described further in Sect. 3.2 and the Supplement.

Two methods were employed to measure the resulting aerosol loading and composition. Particle size distributions between 20 and 800 nm were measured at 85 s time resolution with a scanning electrical mobility sizer (SEMS; BMI Model 2002) consisting of a differential mobility analyzer (BMI Model 2000C) coupled to a water condensation particle counter (TSI Model 3781). Size-dependent aerosol loss rates to the chamber walls were characterized and used to correct size distributions to reflect the total aerosol number and volume concentrations produced in each experiment (McMurry and Grosjean, 1985; VanReken et al., 2006; Fry et al., 2014). This methodology is described in further detail in the Supplement. Aerosol samples from each experiment were collected onto filters (47 mm quartz fiber). Each filter was extracted by sonication in 3 : 1 deionized water : acetonitrile to minimize solvent reactions with analyte compounds (Bateman et al., 2008), and the resulting extract was analyzed offline by high-performance liquid chromatography–electrospray ionization–mass spectrometry (HPLC-ESI-MS).

Due to its relatively soft ionization source and thus minimal fragmentation of analyte compounds, ESI-MS has been employed in several studies to probe SOA composition (Bateman et al., 2008, 2012; Walser et al., 2008; Doezema et al., 2012). The HPLC-ESI-MS system used here consists

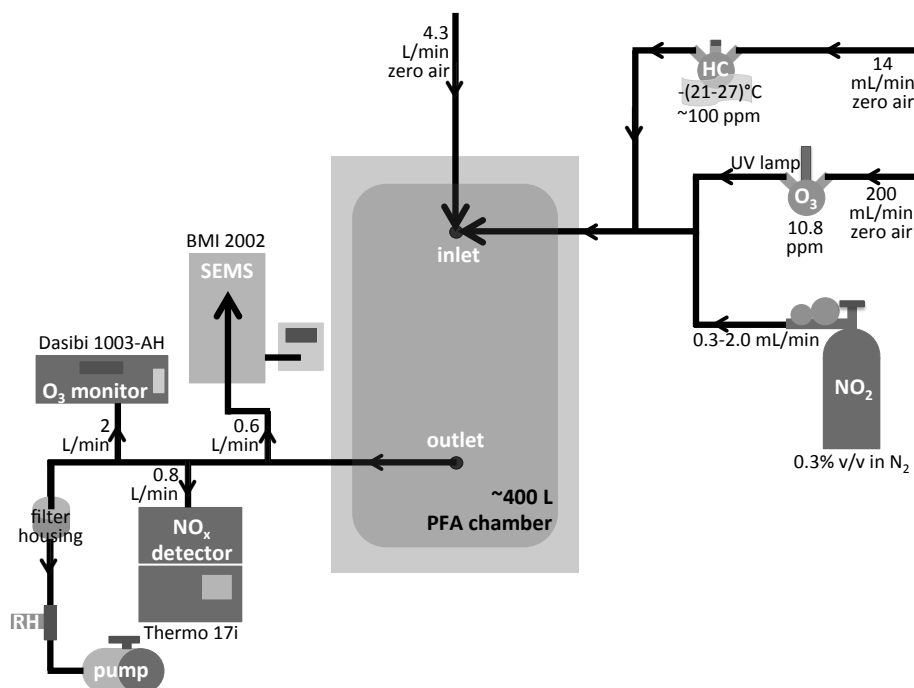


**Figure 2.** Reed environmental chamber (REC) schematic for the experiments described here.

of an Agilent 1100 Series liquid chromatograph coupled to an Agilent LC/MCD TOF G1969A time-of-flight mass spectrometer with an electrospray ionization source. The chromatographic separation occurred on a Kinetex 100 × 3 mm C18 column with 2.6 μm particle size and a sample injection volume of 50 μL at a flow rate of 0.5 mL min<sup>-1</sup>. The electrospray ionization system had a nebulizer gas pressure of 50 psi and an electrospray voltage of 3000 V. High mass resolution ( $m \Delta m^{-1}$  varies between 5000 at  $m/z$  118 amu to 15 000 at  $m/z$  1822 amu) and chromatographic separation of the analytes allowed for straightforward identification of product molecular formulae (Desyaterik et al., 2013).

Between each experiment, the chamber was cleaned for at least 24 h by flushing with zero air and O<sub>3</sub> from the source used during experiments until particle concentrations were at or below their typical background level (< 1 μg m<sup>-3</sup>) and NO<sub>2</sub> concentrations were below 5 ppb. Particle formation was never observed while O<sub>3</sub> and NO<sub>2</sub> were stabilizing for a new experiment, indicating that any traces of BVOC from the previous experiment had been sufficiently removed from the chamber.

### 3 Results and discussion

#### 3.1 Aerosol formation trends

Raw number and volume concentration time series are presented in Fig. 3. These comparisons are not directly indicative of relative yields due to differences in initial monoter-

pene concentrations shown in Table 2 (see Sect. 3.2 for further discussion of aerosol mass yields). However, these comparisons nicely illustrate the vast diversity of the behavior of each monoterpene with respect to systematically changing oxidant conditions, from O<sub>3</sub> dominated to NO<sub>3</sub> dominated. α-Pinene exhibits a decrease in both the total number of particles produced ( $N_{\text{tot}}$ ) and total aerosol volume produced ( $V_{\text{tot}}$ ) with increasing NO<sub>2</sub>, consistent with the findings of other studies (Perraud et al., 2012; Presto et al., 2005). β-Pinene and Δ<sup>3</sup>-carene both exhibit a similar decrease in  $N_{\text{tot}}$  with addition of NO<sub>2</sub> as α-pinene, but at early times in the reaction, the addition of NO<sub>2</sub> appears to enhance volume growth relative to the O<sub>3</sub>-only experiment. Limonene exhibits enhancement in both  $N_{\text{tot}}$  and  $V_{\text{tot}}$  with addition of NO<sub>2</sub>. While all three of the monoalkene monoterpenes produce fewer particles at higher [NO<sub>2</sub>], α-pinene is the only terpene for which the aerosol production seems to be systematically depleted with the addition of NO<sub>2</sub>. β-Pinene and Δ<sup>3</sup>-carene, in contrast, seem to level off at comparable  $N_{\text{tot}}$  values for the intermediate range of [NO<sub>2</sub>]. All four monoterpenes exhibit suppression of aerosol formation at the highest [NO<sub>2</sub>] studied, which is likely the result of RO<sub>2</sub>+NO<sub>2</sub> chemistry becoming kinetically dominant at such high concentrations and producing metastable, less condensable peroxy nitrate products (Barthelmie and Pryor, 1999).

#### 3.2 SOA yields

While this study lacks direct BVOC measurements and thus is not optimized to rigorously measure aerosol yields,

**Table 2.** Conditions for each chamber experiment.

Experiment no.	Date	[BVOC] <sub>i</sub> * (ppb)	[O <sub>3</sub> ] <sub>i</sub> (ppb)	[NO <sub>2</sub> ] <sub>i</sub> * (ppb)	RH (%)	Temp (K)	Notes
<i>α</i> -Pinene							
1	12/19/12	780	485	–	33	294	a
2	1/5/13	680	490	–	20	295	f
3	1/16/13	590–715	480	510	24	294	a, c
4	1/18/13	780–960	480	840	22	295	a, d
5	1/14/13	~ 300	480	1400	22	294	b, e
<i>β</i> -Pinene							
6	1/7/13	370	485	–	40	295	a
7	1/23/13	470–680	480	530	23	295	a, c
8	1/25/13	650–1100	480	910	40	295	a, b, d
9	1/21/13	~ 300	480	2000	20	295	b, e
<i>Δ</i> -Carene							
10	1/9/13	220	470	–	30	294	a
11	3/9/13	250–340	470	290	27	295	a, c
12	3/13/13	400–650	470	590	38	295	a, d
13	2/6/13	~ 300	470	900	33	295	b, e
Limonene							
14	1/11/13	470	485	–	20	295	a
15	3/23/13	340–400	470	360	20	295	a, c
16	3/27/13	470–560	470	720	31	295	a, d
17	3/21/13	~ 300	465	1000	26	295	a, b, e

\* Values calculated using kinetics model. <sup>a</sup> SOA filter sample collected and analyzed by HPLC-ESI-MS. <sup>b</sup> [BVOC] estimated according to flow rate and temperature-dependent vapor pressure within source flask. <sup>c</sup> Designated “low NO<sub>2</sub>.” <sup>d</sup> Designated “medium NO<sub>2</sub>.” <sup>e</sup> Designated “high NO<sub>2</sub>.” <sup>f</sup> Experiment included to show reproducibility of chamber.

the framework of aerosol mass yields can still be used to compare aerosol formation trends between each experiment while accounting for differing initial hydrocarbon concentrations as well as differing aerosol mass loadings for each experiment. Unitless aerosol mass yields ( $Y$ ) are defined as the aerosol mass produced per hydrocarbon mass consumed ( $Y = \Delta M / \Delta \text{HC}$ ). Since the hydrocarbon was not measured online during experiments,  $\Delta \text{HC}$  values were determined using the gas-phase kinetics model described in detail in the Supplement. The modeled cumulative concentration of monoterpene reacted was converted to  $\Delta \text{HC}$  in  $\mu\text{g m}^{-3}$  using the molecular weight of monoterpenes ( $136.23 \text{ g mol}^{-1}$ ). In the model,  $\Delta \text{HC}$  is calculated based on how much of each oxidant reacts with the monoterpene. However, NO<sub>3</sub> can also react with subsequent RO<sub>2</sub> radicals, thus depleting the concentration available to react directly with BVOC. The rate constant used for RO<sub>2</sub> + NO<sub>3</sub> ( $2 \times 10^{-12} \text{ cm}^3 \text{ molec}^{-1} \text{ s}^{-1}$ ) is reasonably well known and constant over a range of RO<sub>2</sub> structures ( $1.8 \pm 1.5 \times 10^{-12} \text{ cm}^3 \text{ molec}^{-1} \text{ s}^{-1}$  for C<sub>2</sub> - C<sub>6</sub> RO<sub>2</sub>) (Vaughan et al., 2006). The rate constant for RO<sub>2</sub> + RO<sub>2</sub>, the main competing RO<sub>2</sub> sink, is far more variable over RO<sub>2</sub> structures, though, so the “best estimate” employed in this study spans 3 orders of magnitude (described further in

Supplement). Therefore,  $k_{\text{RO}_2+\text{RO}_2}$  is the largest source of uncertainty in  $\Delta \text{HC}$ , and aerosol yield ranges are calculated spanning the minimum ( $10^{-15} \text{ cm}^3 \text{ molec}^{-1} \text{ s}^{-1}$ ) and maximum ( $10^{-12} \text{ cm}^3 \text{ molec}^{-1} \text{ s}^{-1}$ ) values used. Because O<sub>3</sub> is not expected to react with RO<sub>2</sub> (whereas NO<sub>3</sub> does),  $\Delta \text{HC}$  from the O<sub>3</sub>-only experiments does not vary in response to shifting  $k_{\text{RO}_2+\text{RO}_2}$  values.

$\Delta M$  was determined by converting the wall-loss-corrected aerosol total volume data to mass, assuming a SOA density of  $1.4 \text{ g mL}^{-1}$  (Hoyle et al., 2011). Uncertainty in  $\Delta M$  was estimated using replicate measurements of *α*-pinene + O<sub>3</sub> (experiments 1 and 2 in Table 2) as described in detail in the Supplement. The two  $\Delta M$  time series were interpolated onto the same  $\Delta \text{HC}$  trace, and time series of the average and standard deviation of  $\Delta M$  were calculated. The deviation between these two experiments was slightly variable with time, so we conservatively chose the highest stable value – 15 % relative error – to use as the  $\Delta M$  precision estimate. Using the corresponding  $\Delta M$  and  $\Delta \text{HC}$  time series and respective uncertainties, a time series of mass yields was attainable, as shown in Fig. 4, plotted against aerosol mass produced ( $\Delta M$ ), where  $\Delta M$  and  $\Delta \text{HC}$  are calculated relative to the beginning of the experiment. In some cases, namely the *β*-

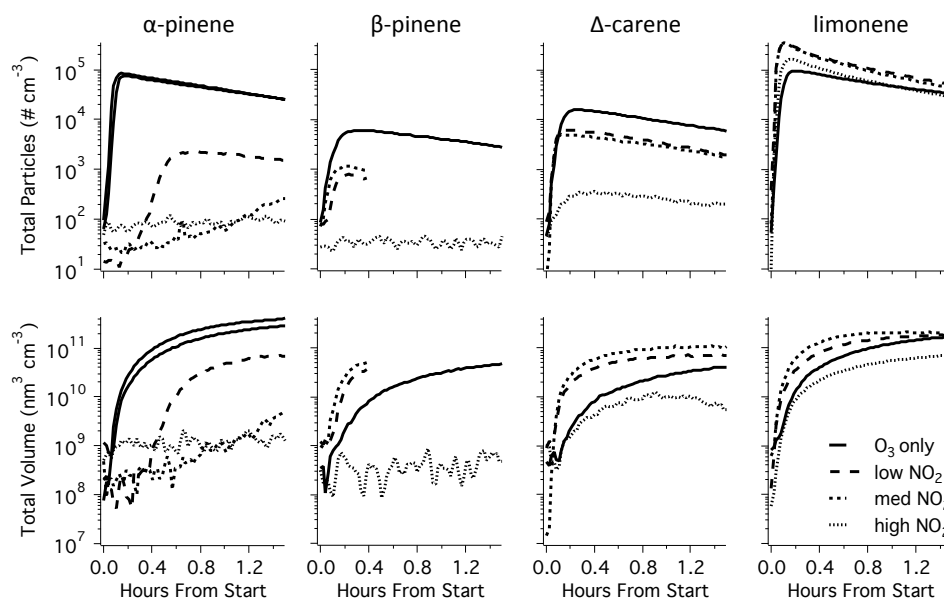


**Figure 3.** Raw total number concentrations ( $N_{\text{tot}}$ ) and total volume concentrations ( $V_{\text{tot}}$ ) at each NO<sub>2</sub> concentration for each monoterpene studied, not corrected for wall losses.

pinene + O<sub>3</sub> + NO<sub>2</sub> experiments, the aerosol growth rapidly exceeded the size range of the SEMS (20–800 nm). Aerosol data presented here are truncated as soon as the size distribution begins to exceed the range of the SEMS instrument resulting in these experiments “ending” at quite low mass loadings before the yield curves have flattened.

A variety of factors may contribute to the absolute numerical values of these yields differing from yields reported in the literature. For example, vapor-phase wall losses were not accounted for (Zhang et al., 2014), and the chamber size, mixing, and conditioning of walls differ from other studies. Since these experiments were conducted without seed particles, rather than having a constant particle distribution for vapors to condense onto, size distributions emerged as freshly nucleated particles that proceeded through full growth curves until they exceeded the range of the SEMS and eventually were removed through the constant outflow of the chamber. This combination of growth and dilution led to an oscillatory behavior of periodic full growth curves as the condensational sink was changing, thus preventing a true steady state from ever being achieved. The yield curves shown in Fig. 4 highlight a single growth curve for each experiment, but these yields may be more indicative of kinetically limited growth than thermodynamic partitioning, causing them to differ from other studies. Additionally, and perhaps most importantly, the chemistry itself (including both first-generation oxidation and peroxy radical fate) is expected to differ substantially in these mixed oxidant conditions compared to single oxidant studies in the literature. With all of those factors in mind, the precision reflected in the error ranges in Fig. 4 gives us confidence that the relative yield comparisons between individual experiments in this study are robust.

Figure 4 enables yield comparisons at comparable mass loadings and also accounts for the fact that each experiment began with somewhat variable BVOC concentrations. We still see similar trends as were observed in the  $V_{\text{tot}}$  panels of Fig. 3. Figure 4 illustrates that increasing [NO<sub>2</sub>] substantially depletes aerosol formation from  $\alpha$ -pinene, whereas  $\beta$ -pinene and  $\Delta^3$ -carene have comparable yields over the full range of oxidant conditions, and limonene exhibits enhancement of aerosol formation at higher [NO<sub>2</sub>]. It should be noted that yield calculations were only performed on the O<sub>3</sub>-only and lowest two [NO<sub>2</sub>] studied for each monoterpene due to difficulties in reliably reproducing  $\Delta\text{HC}$  in the kinetics model for the highest [NO<sub>2</sub>] experiments. The model is constrained using the observed O<sub>3</sub> decay, but these high NO<sub>2</sub> experiments react nearly all the BVOC by way of NO<sub>3</sub>, leaving the O<sub>3</sub> decay nearly unaffected. Furthermore, we expect the full duration of these experiments to be kinetically dominated by the RO<sub>2</sub>+NO<sub>2</sub> reservoir (peroxy nitrates), thus hindering SOA production. For these reasons, the high NO<sub>2</sub> experiments are not included in yield comparisons.

### 3.3 Individual oxidant contributions

Gas-phase kinetics modeling of the steady-state conditions in the chamber yielded the time series of relative O<sub>3</sub> and NO<sub>3</sub> (and OH) contributions to BVOC oxidation. Since each experiment starts with O<sub>3</sub>, NO<sub>2</sub>, NO<sub>3</sub>, and N<sub>2</sub>O<sub>5</sub> at their equilibrium concentrations, initial BVOC oxidation will be dominated by NO<sub>3</sub>, which reacts orders of magnitude faster than O<sub>3</sub> (Table 1). Eventually, as concentrations of precursors change over time, rates to each oxidant change and O<sub>3</sub> starts to contribute. We assume OH is produced from sta-

**Table 3.** Percentage of total BVOC reacted by each oxidant at 2 h into each experiment. In the model, OH is produced from stabilized Criegee intermediates from ozonolysis at the following ratios:  $\alpha$ -pinene = 0.85;  $\beta$ -pinene = 0.35;  $\Delta^3$ -carene = 1.06; limonene = 0.86 (Atkinson et al., 1992). Values from NO<sub>2</sub>-containing experiments include two values expressed as low/high where “low” denotes the lower RO<sub>2</sub> + RO<sub>2</sub> rate constant limit ( $10^{-15}$  cm<sup>3</sup> molec<sup>-1</sup> s<sup>-1</sup>) and “high” denotes the upper limit ( $10^{-12}$  cm<sup>3</sup> molec<sup>-1</sup> s<sup>-1</sup>) as described in the Supplement.

	[NO <sub>2</sub> ] <sub>i</sub> (ppb)	% by NO <sub>3</sub>	% by O <sub>3</sub>	% by OH
$\alpha$ -Pinene	0	0	54	46
	510	44 (68)	34 (21)	22 (11)
	840	58 (78)	26 (15)	16 (7)
$\beta$ -Pinene	0	0	74	26
	530	77 (94)	18 (5)	5 (1)
	910	81 (95)	15 (4)	4 (1)
$\Delta^3$ -Carene	0	0	49	51
	290	62 (92)	21 (5)	17 (3)
	590	63 (95)	20 (4)	17 (1)
Limonene	0	0	54	46
	360	45 (74)	34 (18)	21 (8)
	720	59 (85)	26 (11)	15 (4)

bilized Criegee intermediates from ozonolysis according to the monoterpene-dependent yields found in Atkinson et al. (1992) and described in the Supplement. The timing and relative contribution of O<sub>3</sub> depends on the relative rate constants of O<sub>3</sub> and NO<sub>3</sub> with each monoterpene and thus the influence of each oxidant varies for all conditions tested.

This feature of staggered oxidant contributions is convenient to test the hypothesis that observed yield differences between different oxidant conditions applied to a single monoterpene can be attributed to distinct contributions from NO<sub>3</sub> and O<sub>3</sub> oxidation. For  $\beta$ -pinene (Fig. 5),  $\Delta^3$ -carene (Fig. S8), and limonene (Fig. S8), the fact that any aerosol mass is observed during the beginning of the NO<sub>2</sub> experiments when oxidation exclusively goes by way of NO<sub>3</sub> indicates that qualitative yield differences relative to the O<sub>3</sub> experiment can be attributed at least in part to NO<sub>3</sub> oxidation products. In contrast, Fig. 5 shows that neither of the  $\alpha$ -pinene experiments with NO<sub>2</sub> produce any aerosol mass until O<sub>3</sub> starts to contribute. This observation is consistent with the hypothesis that the observed suppression of aerosol formation from  $\alpha$ -pinene with increasing concentrations of NO<sub>2</sub> can be attributed to its (near) 0% yield with NO<sub>3</sub> observed in other studies (Hallquist et al., 1999; Spittler et al., 2006; Fry et al., 2014).

For  $\beta$ -pinene,  $\Delta^3$ -carene, and limonene, while it is clear that aerosol mass forms from NO<sub>3</sub> oxidation products in the NO<sub>2</sub> experiments, a time lag becomes apparent during which BVOC is reacting but no aerosol is formed. As soon as aerosol formation is initiated, however, the mass rapidly increases. The kinetics model used in this study assumes three options for RO<sub>2</sub> fate: reaction with RO<sub>2</sub>, NO<sub>3</sub>, or NO<sub>2</sub>. In Sect. 3.1, we propose that high NO<sub>2</sub> experiments yield low mass concentrations due to the formation of less sta-

ble peroxy nitrates. This explanation likely accounts for the lag time observed in each NO<sub>2</sub> experiment before aerosol is able to form. Indeed, from the model we can calculate a ratio of RO<sub>2</sub> + NO<sub>2</sub> products relative to the sum of RO<sub>2</sub> + RO<sub>2</sub>, RO<sub>2</sub> + NO<sub>3</sub>, and RO<sub>2</sub> + NO<sub>2</sub> products present in the chamber at each time in the experiment. When this ratio time series is overlaid onto the plots in Fig. 5, a minimum in RO<sub>2</sub> + NO<sub>2</sub> products appears at approximately the same time that aerosol formation is initiated. This timing, shown in Fig. 5 and Fig. S8, indicates that even the low NO<sub>2</sub> experiments have enough NO<sub>2</sub> present that formation of relatively volatile peroxy nitrates may kinetically dominate experiments at early times until RO<sub>2</sub> + RO<sub>2</sub> and RO<sub>2</sub> + NO<sub>3</sub> products start to compete.

The percentage of BVOC reacted by each of the three oxidants was modeled and is shown in Table 3. Comparisons were made 2 h into the reaction after the initial buildup of NO<sub>3</sub> and N<sub>2</sub>O<sub>5</sub> was depleted and chemical production of NO<sub>3</sub> more realistically competes with O<sub>3</sub> oxidation of BVOCs. Even at this point in time, NO<sub>3</sub> dominates the initial oxidation pathway for all NO<sub>2</sub> concentrations and all monoterpenes, further indicating that if NO<sub>3</sub> oxidation contributes to SOA mass, as is certainly the case for  $\beta$ -pinene,  $\Delta^3$ -carene, and limonene, these NO<sub>3</sub> oxidation products are plentiful enough throughout the full experiment to contribute significantly to observed yield differences between those experiments relative to the O<sub>3</sub>-only experiments.

### 3.4 Bulk SOA composition

Filter samples from experiments that yielded sufficient aerosol mass (all experiments in Table 2 except 1, 5, 9, 13) were collected and analyzed offline by HPLC-ESI-MS at

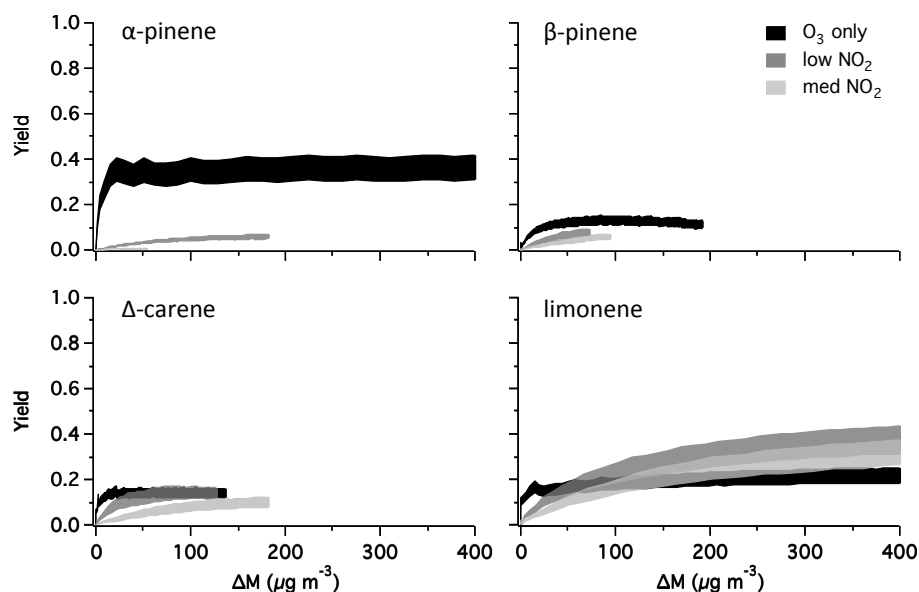


**Figure 4.** Yield vs.  $\Delta M$  for each experiment.  $\Delta M$  is corrected for wall losses (described in Supplement). Uncertainty ranges on yields arise from a constant 15% relative error on  $\Delta M$  calculated based on two replicate experiments, propagated with modeled  $\Delta H C$  values using the range of  $10^{-15}$  to  $10^{-12}$   $\text{cm}^3 \text{molec}^{-1} \text{s}^{-1}$  for  $k_{\text{RO}_2+\text{RO}_2}$  for the low and medium NO<sub>2</sub> experiments for each monoterpene. O<sub>3</sub>-only experiments do not have an analogous  $\Delta H C$  uncertainty range since all O<sub>3</sub> was assumed to react with the monoterpene directly, so uncertainty range on these traces is based exclusively on  $\Delta M$ .

Colorado State University. Because electrospray ionization is a soft ionization technique, this method has been shown to be especially useful for detecting a wide range of  $m/z$  products – including oligomer species that are likely to be significant SOA constituents (Walser et al., 2008; Surratt et al., 2006; Doezema et al., 2012). Although quantitative comparisons of products are not possible due to differences in mass loadings and a lack of calibration standards, qualitative differences in product distributions were readily apparent and consistent with observed aerosol yield trends.

Introducing NO<sub>2</sub> into ozonolysis of monoterpenes influences the composition of resulting SOA in two different ways: first, by forming NO<sub>3</sub> that can either oxidize BVOC directly or react with NO<sub>3</sub>- or O<sub>3</sub>-initiated RO<sub>2</sub>, or second, by directly reacting with RO<sub>2</sub> or other products and reaction intermediates as NO<sub>2</sub>. A visual comparison of the total ion chromatograms from ozonolysis of  $\beta$ -pinene with no NO<sub>2</sub> and the two lowest concentrations of NO<sub>2</sub> (Fig. 6) shows that several new products form once NO<sub>2</sub> is added, and that in general increasing [NO<sub>2</sub>] simply increases the intensity of those products rather than changing product identities substantially. For ease of interpretation, results from all of the NO<sub>2</sub>-containing experiments were combined into a single product distribution from “NO<sub>3</sub>-influenced oxidation.” We can then compare those product distributions to those of the O<sub>3</sub>-only experiments. A complete list of compound formulae detected (> 1.5% relative intensity, see Supplement) in the O<sub>3</sub> and NO<sub>3</sub> dominated oxidation of each monoterpene is compiled in Table S2.

To best highlight qualitative differences in the identity of molecules that make SOA for each set of precursors, every unique compound (distinct either in mass, retention time, or both) was accounted for once, not normalized by peak intensity. A variety of average bulk composition parameters were calculated for each experiment, highlighted in Table 4, including average number of C, O, and N atoms per compound, molecular weight, and total number of products. Some artifacts may remain in this data set, such as impurities not captured by the background subtraction or product fragments that do not reflect the original identity of the SOA product. The former should affect all samples uniformly in this analysis and thus will not influence qualitative comparisons, and the latter will either affect multiple samples and thus be irrelevant in comparisons or only affect single samples and thus still provide interesting qualitative differences.

A direct correlation between any of the average parameters ( $MW_{\text{avg}}$ ,  $C_{\text{avg}}$ ,  $O_{\text{avg}}$ ,  $N_{\text{avg}}$ ) in Table 4 and absolute aerosol yields is not obvious.  $\alpha$ -Pinene ozonolysis, for example, produced the highest aerosol mass of all the conditions tested, and while its average MW and number of C atoms are higher than ozonolysis from all the other monoterpenes, those same values are comparable to each of the NO<sub>3</sub> experiments and substantially lower than those values for limonene + NO<sub>3</sub>. However, the difference in average values, defined as the difference in each average parameter between O<sub>3</sub> and NO<sub>3</sub> dominated oxidation for each monoterpene ( $\Delta_{\text{avg}}$ ), are consistent with O<sub>3</sub> vs. NO<sub>3</sub> yield comparisons.  $\beta$ -Pinene and  $\Delta^3$ -carene have similar  $\Delta_{\text{avg}}$  values for each parameter (as



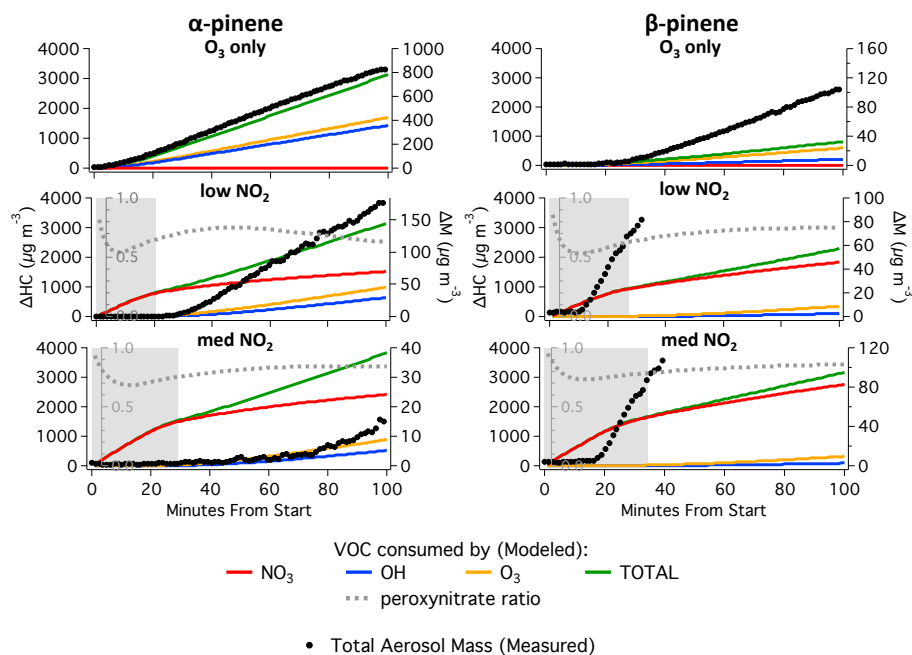


**Figure 5.** Time series of wall-loss-corrected aerosol mass (right axis) and VOC consumed by each oxidant (left axis) for  $\alpha$ -pinene and  $\beta$ -pinene at 0 (“O<sub>3</sub>-only”), low, and medium NO<sub>2</sub> concentrations, highlighting how much aerosol is produced at times dominated by NO<sub>3</sub> oxidation (shaded regions).  $\Delta$ Hc values shown are the lower limits calculated using the lowest RO<sub>2</sub>+RO<sub>2</sub> rate constant ( $10^{-15}$  cm<sup>3</sup> molec<sup>-1</sup> s<sup>-1</sup>), which gives the low limit on how much NO<sub>3</sub> reacts with VOC directly. Dashed grey traces (inner left grey axis) represent the ratio of RO<sub>2</sub>+NO<sub>2</sub> products that are present in the chamber (instantaneous concentration) relative to the sum of the instantaneous concentrations of RO<sub>2</sub>+NO<sub>2</sub>, RO<sub>2</sub>+NO<sub>3</sub>, and RO<sub>2</sub>+NO<sub>2</sub> products. This ratio is a representation of the time dependence of peroxy nitrate formation in the chamber.

well as similar absolute values for each oxidant condition), suggesting that the addition of NO<sub>3</sub> affects the product distribution of these two monoterpenes similarly. The  $\Delta_{\text{avg}}$  values for limonene are much higher than any other monoterpene in this study, consistent with it having the highest NO<sub>3</sub> aerosol yields. Again, perhaps most notably, the  $\Delta_{\text{avg}}$  parameters hover near 0 for  $\alpha$ -pinene, suggesting that the aerosol composition does not differ much between the two oxidants – consistent with all of  $\alpha$ -pinene’s aerosol production coming exclusively from O<sub>3</sub> oxidation.

To illustrate some of the finer detail of these product distributions, Fig. 7 shows histograms where each observed product is binned by compound mass in 50 amu intervals. Every experiment shows some contribution from oligomer products ( $m/z > 246$  according to Perraud et al. (2010);  $> 300$  according to Walser et al., 2008), but this contribution is most pronounced from NO<sub>3</sub> oxidation of  $\beta$ -pinene,  $\Delta^3$ -carene, and limonene. In particular, we observe substantially more distinct products  $> 400$  amu from  $\beta$ -pinene,  $\Delta^3$ -carene, and limonene with the O<sub>3</sub>/NO<sub>2</sub>/NO<sub>3</sub> mixture than from O<sub>3</sub> alone. In this region, the mass distributions for  $\alpha$ -pinene in both oxidant conditions are identical. Since mass is an important contributing factor to volatility (e.g., Donahue et al., 2011), these high-mass products are likely important in aerosol formation and growth and thus may be explana-

tory of the observed yield differences from NO<sub>3</sub> oxidation. If oligomerization is an important pathway leading to SOA formation and growth from NO<sub>3</sub>-initiated chemistry,  $\alpha$ -pinene’s lack of oligomer products with NO<sub>3</sub> may be responsible for its 0% aerosol yield. In contrast, comparison of the four O<sub>3</sub>-only histograms shows relatively small contributions of high MW oligomers for any monoterpene, in spite of quite high aerosol yields in some cases, indicating that aerosol formation by ozonolysis may not require oligomerization.

Recent studies of SOA nucleation and growth from ozonolysis of  $\alpha$ -pinene have shown that highly oxidized and/or oligomeric species are likely important in nucleation and early growth, but that growth beginning around 20 nm is dominated by lower MW products (140–380 amu) (Zhao et al., 2013; Winkler et al., 2012). This latter MW range is consistent with the ozonolysis products we observe for all four monoterpenes, indicating that high MW products may dominate only early stages of growth and are thus not detectable at the high-mass loadings in this study. NO<sub>3</sub> oxidation, however, seems to provide a weaker source of low volatility compounds contributing to nucleation and early growth, as seen in the decrease of  $N_{\text{tot}}$  with increasing [NO<sub>2</sub>] in Fig. 3 (with the exception of limonene), but produces oligomers throughout the full time period of aerosol growth, leading to total aerosol mass concentrations that rival ozonol-

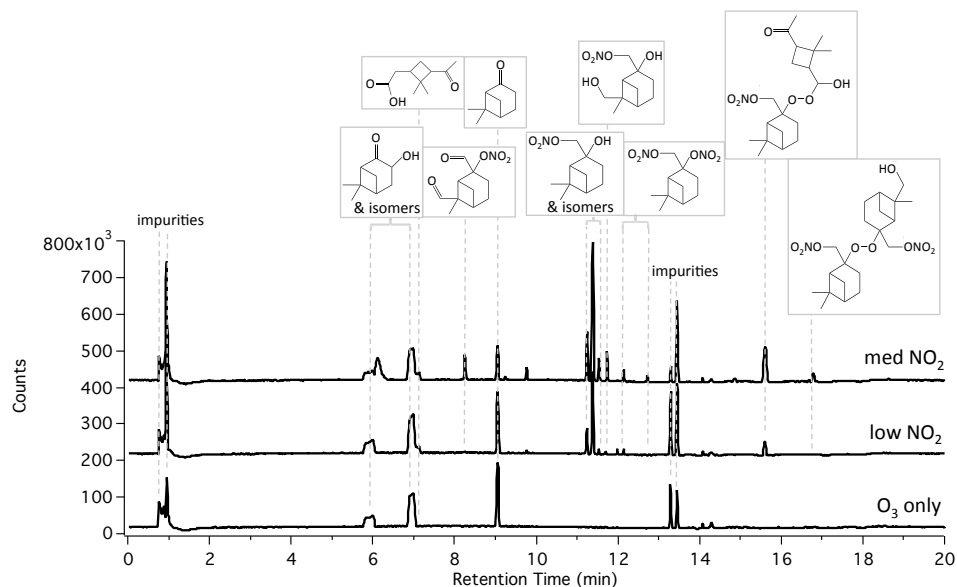


**Figure 6.** Comparison of chromatograms from HPLC-ESI-MS samples of SOA derived from  $\beta$ -pinene ozonolysis with 0 (bottom), 530 (middle), and 910 ppb NO<sub>2</sub> (top). Chromatograms are annotated with speculative structures corresponding to the assigned molecular formulae of the most intense peaks. Proposed structures are listed in Table S3 based on products observed in other studies.

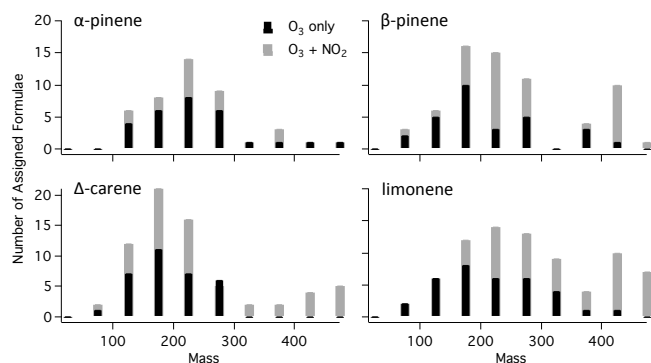


**Figure 7.** Histograms of each O<sub>3</sub> vs. NO<sub>3</sub> (O<sub>3</sub> + NO<sub>2</sub>) regime for each monoterpene showing the number of compounds (left axis) in each 50 amu mass bin (bottom axis).

ysis (with the exception of  $\alpha$ -pinene), as seen in Fig. 4. Further supporting this observed difference in products from ozonolysis compared to NO<sub>3</sub> oxidation is the difference in the reaction rate of each process. O<sub>3</sub> + BVOC is much slower than NO<sub>3</sub> + BVOC, which means that RO<sub>2</sub> is produced more slowly from ozonolysis and thus the RO<sub>2</sub> lifetime is much longer with respect to other radical species. Longer RO<sub>2</sub> lifetimes are more conducive to isomerization processes like autoxidation (Crouse et al., 2013; Jokinen et al., 2014), which may be responsible for the initial high MW nucleating species observed in other ozonolysis studies. In contrast, NO<sub>3</sub> oxidation produces RO<sub>2</sub> much more rapidly, therefore increasing the likelihood of RO<sub>2</sub> + RO<sub>2</sub> oligomerization.

Mass spectra alone provide limited compositional information since they do not distinguish between different functional groups. However, in this system, one functional group that can be easily parsed out of the data is the nitrate group. From the NO<sub>3</sub> initiated oxidation chemistry, we expect that any nitrogen present in a molecule is a part of a nitrate functional group. (Some instances of –NO and –ONO have been found in the compound list, causing relatively high  $N_{\text{avg}}$  values for  $\alpha$ -pinene + O<sub>3</sub>, for example, where we expect any nitrogen is due to impurities.) The  $\Delta_{\text{avg}}$  values in Table 4 for  $N_{\text{avg}}$  provide an approximate estimate of relative aerosol organic nitrate yield.  $\beta$ -Pinene,  $\Delta^3$ -carene, and limonene all exhibit a substantial increase in average number of N per molecule with the addition of NO<sub>2</sub>, consistent with the relatively high organic nitrate yields observed from NO<sub>3</sub> oxidation of those species in other studies (Fry et al., 2014; Hallquist et al., 1999).  $\alpha$ -Pinene produces comparatively fewer nitrogen-containing SOA products in the presence of NO<sub>2</sub>. While the organic nitrate products from  $\alpha$ -pinene may be relatively volatile and thus not partition appreciably into the aerosol phase, it is clear that this is not a universal characteristic of C<sub>10</sub> organic nitrates, as many do partition into the aerosol phase for all three other monoterpenes studied – even those with relatively low total aerosol mass loading.

We note that the products observed here from ozonolysis vs. NO<sub>3</sub> oxidation are consistent with proposed mechanisms in the literature. Table S3 includes proposed structures for several masses that have been observed in other studies, including several monomeric carboxylic acids and aldehydes from ozonolysis (Glasius et al., 2000; Yu et al., 1999) as well as multi-functional monomeric nitrates from NO<sub>3</sub> oxidation

**Table 4.** Average ( $\pm 1$  standard deviation) molecular weight, number of C, O, and N atoms, O / C, and total number of products identified by HPLC-ESI-MS analysis of aerosol collected from O<sub>3</sub> and NO<sub>3</sub> (O<sub>3</sub> + NO<sub>2</sub> + NO<sub>3</sub>) oxidation of each monoterpene studied. The difference in average value for each parameter ( $\Delta_{\text{avg}}$ ) from each oxidation scheme was also tabulated for each monoterpene.

	$\alpha$ -Pinene			$\beta$ -Pinene		
	O <sub>3</sub>	NO <sub>3</sub>	$\Delta_{\text{avg}}$	O <sub>3</sub>	NO <sub>3</sub>	$\Delta_{\text{avg}}$
MW <sub>avg</sub>	237.6 $\pm$ 86.9	233.9 $\pm$ 81.0	-3.7	212.0 $\pm$ 88.9	249.3 $\pm$ 104.3	37.3
C <sub>avg</sub>	13.8 $\pm$ 5.4	13.2 $\pm$ 5.0	-0.6	12.0 $\pm$ 4.5	12.7 $\pm$ 4.7	0.7
O <sub>avg</sub>	2.9 $\pm$ 1.6	3.1 $\pm$ 1.7	0.2	2.9 $\pm$ 2.1	4.2 $\pm$ 2.6	1.3
N <sub>avg</sub>	0.29 $\pm$ 0.53	0.40 $\pm$ 0.58	0.11	0.14 $\pm$ 0.36	0.74 $\pm$ 0.73	0.60
O / C	0.22 $\pm$ 0.11	0.25 $\pm$ 0.14	0.03	0.23 $\pm$ 0.12	0.32 $\pm$ 0.16	0.09
# ID'd	28	43	15	29	66	37
	$\Delta$ -Carene			Limonene		
	O <sub>3</sub>	NO <sub>3</sub>	$\Delta_{\text{avg}}$	O <sub>3</sub>	NO <sub>3</sub>	$\Delta_{\text{avg}}$
MW <sub>avg</sub>	191.7 $\pm$ 56.9	232.1 $\pm$ 111.5	40.4	216.9 $\pm$ 81.2	306.5 $\pm$ 128.6	89.6
C <sub>avg</sub>	11.0 $\pm$ 3.1	12.4 $\pm$ 4.7	1.4	12.3 $\pm$ 4.2	14.7 $\pm$ 4.8	2.4
O <sub>avg</sub>	2.4 $\pm$ 1.2	3.6 $\pm$ 3.0	1.2	2.9 $\pm$ 1.8	5.9 $\pm$ 4.0	3.0
N <sub>avg</sub>	0.09 $\pm$ 0.30	0.41 $\pm$ 0.67	0.32	0.18 $\pm$ 0.46	0.94 $\pm$ 1.06	0.76
O / C	0.22 $\pm$ 0.11	0.27 $\pm$ 0.14	0.05	0.23 $\pm$ 0.13	0.39 $\pm$ 0.23	0.16
# ID'd	32	70	38	34	85	51

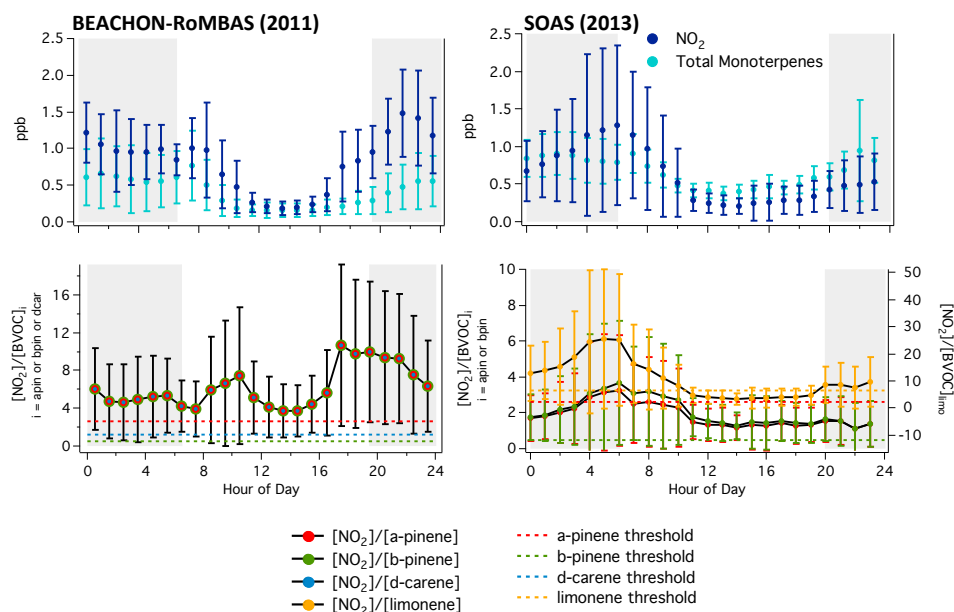


**Figure 8.** Diurnal average NO<sub>2</sub> and monoterpene concentrations (top panels) are shown for two field campaigns: BEACHON-RoMBAS 2011 (left panels) and SOAS 2013 (right panels) which both occurred at heavily biogenically influenced sites. The bottom panels show the diurnally averaged [NO<sub>2</sub>]/[BVOC] ratios for the speciated monoterpenes used in this study. The speciated monoterpenes for BEACHON-RoMBAS are estimated as being 1 : 1 : 1  $\alpha$ -pinene :  $\beta$ -pinene :  $\Delta^3$ -carene; hence, each BVOC concentration is assumed to be a third of total measured [BVOC]. Shaded regions indicate nighttime hours.

(Wangberg et al., 1997; Perraud et al., 2010), some of which have been included in Fig. 6 to highlight relative intensities across different NO<sub>2</sub> conditions. Several more speculative structures are shown in the Supplement to indicate that observed oligomeric masses can be reasonably achieved from dimers of first-generation oxidation products.

#### 4 Implications: determination of dominant nighttime oxidant using NO<sub>2</sub> to BVOC ratio

Using literature rate constant data (Table 1), we can approximate the NO<sub>2</sub>/BVOC regime where NO<sub>3</sub> will dominate nighttime oxidation for each monoterpene. Since O<sub>3</sub> contributes to both NO<sub>3</sub> formation and BVOC oxidation, and

**Table 5.** Minimum [NO<sub>2</sub>]/[BVOC] value reported for each monoterpene studied at which NO<sub>3</sub> is expected to dominate nighttime oxidation.

BVOC	[NO <sub>2</sub> ]/[BVOC]
$\alpha$ -Pinene	2.6
$\beta$ -Pinene	0.47
$\Delta^3$ -Carene	1.2
Limonene	6.6

for all monoterpenes NO<sub>3</sub> oxidation is much faster than O<sub>3</sub> oxidation, we assume that once NO<sub>3</sub> production becomes faster than O<sub>3</sub> oxidation of BVOC (Eq. 1), NO<sub>3</sub> becomes the dominant oxidant. The ratio of NO<sub>2</sub>/BVOC at which this crossover occurs, defined in Eq. (2), is calculated for each monoterpene and reported in Table 5.

$$k_{(\text{O}_3+\text{NO}_2)}[\text{O}_3][\text{NO}_2] > k_{(\text{O}_3+\text{BVOC})}[\text{O}_3][\text{BVOC}], \quad (1)$$

$$\frac{[\text{NO}_2]}{[\text{BVOC}]} > \frac{k_{(\text{O}_3+\text{BVOC})}}{k_{(\text{O}_3+\text{NO}_2)}}. \quad (2)$$

This calculation leaves out factors like competing sinks for NO<sub>3</sub> and is thus a very crude approximation. Nevertheless, it is noteworthy how small the magnitude of these ratios are. Figure 8 shows diurnally averaged NO<sub>2</sub> and bulk monoterpene concentrations from two field campaigns: BEACHON-RoMBAS in 2011, which took place in a remote montane forested location in the Rocky Mountain front range (Fry et al., 2013), and SOAS in 2013, which took place in a rural subtropical forest region in central Alabama (Ayles et al., 2015). Across both of these campaigns, NO<sub>2</sub> and total monoterpene diurnal concentrations were qualitatively and quantitatively similar. For the BEACHON-RoMBAS campaign, we assume that the average monoterpene distribution was 1 : 1 : 1  $\alpha$ -pinene :  $\beta$ -pinene :  $\Delta^3$ -carene (Fry et al., 2013), whereas at SOAS we have explicit speciated monoterpene measurements. For each campaign, we calculated the average diurnal cycle of [NO<sub>2</sub>]/[BVOC] using speciated monoterpene concentrations. The dashed lines indicate the minimum calculated threshold from Table 5, above which NO<sub>3</sub> oxidation is expected to dominate over O<sub>3</sub> oxidation. The shaded nighttime portions of Fig. 8 show measured average [NO<sub>2</sub>]/[BVOC] ratios exceeding the minimum threshold at all times during the BEACHON-RoMBAS campaign and at all times for  $\beta$ -pinene and limonene at SOAS as well as part of the night for  $\alpha$ -pinene at SOAS.

These ratios are expected to be even higher in regions with stronger anthropogenic influences. This analysis suggests that NO<sub>3</sub> is not only a relevant contributor to nighttime oxidation chemistry, it may actually dominate oxidation pathways in many regions. The consequence of this NO<sub>3</sub>-dominant oxidation chemistry for SOA formation downwind of large NO<sub>x</sub> point sources (coal-fired power plants) has been recently investigated (Fry et al., 2015), showing spatial pat-

terns of predicted SOA production that depend substantially on the forest surrounding the point source. The present study expands on this thinking to include further downwind regions where O<sub>3</sub> and NO<sub>3</sub> begin to compete. If NO<sub>3</sub> contributes significantly to oxidation pathways in ambient air over a wide range of NO<sub>2</sub> concentrations, the fact that each monoterpene displays vastly different aerosol yields from NO<sub>3</sub> vs. O<sub>3</sub> oxidation and that this difference differs among monoterpenes becomes essential to accurately predicting aerosol formation in different regions.

## 5 Conclusions

This work adds to the growing body of monoterpene aerosol yield comparison literature suggesting that monoterpene oxidation has widely varying aerosol yields depending on the specific monoterpene and oxidant combination (Fry et al., 2014; Griffin et al., 1999; Hallquist et al., 1999; Ng et al., 2006; Glasius et al., 2000; Yu et al., 1999; Lee et al., 2006). We therefore conclude, first and foremost, that there is no single “representative” monoterpene. Furthermore, the monoterpene most often considered representative of BVOC oxidation,  $\alpha$ -pinene, presents here as the greatest anomaly with respect to aerosol formation, showing higher ozonolysis aerosol mass yields than even limonene, and behaving in a way consistent with 0 % aerosol yields from reaction with NO<sub>3</sub>.

We show that under the influence of NO<sub>3</sub>,  $\alpha$ -pinene produces comparatively few condensed-phase organic nitrates and oligomers with respect to the other three monoterpenes studied. This finding is consistent with  $\alpha$ -pinene’s negligible aerosol yield with NO<sub>3</sub> and also suggests more generally that oligomers and multifunctional organic nitrates are important products leading to SOA formation from NO<sub>3</sub>. Additionally, the difference in product distributions between O<sub>3</sub> and NO<sub>3</sub> oxidation for all monoterpenes studied (except  $\alpha$ -pinene) indicates that each oxidant broadly employs a different mechanism toward condensable products – O<sub>3</sub> likely nucleates and grows enough aerosol mass early in the reaction that subsequent condensation is governed by comparatively small molecular weight species, whereas NO<sub>3</sub> produces less extremely low-volatility material early but produces oligomers consistently throughout the period of condensation such that they constitute an observable fraction of the bulk aerosol.

Careful treatment of the first-generation kinetics of this atmospherically relevant nighttime oxidant mixture also served to contextualize the relative importance of each observed aerosol precursor in different regions. We propose using NO<sub>2</sub>/BVOC ratios for each monoterpene to predict the dominant nighttime oxidation pathway for each (Table 5). For example, for  $\beta$ -pinene at NO<sub>2</sub>/BVOC ratios greater than 0.47, NO<sub>3</sub> oxidation will begin to out-compete O<sub>3</sub> oxidation, suggesting that  $\beta$ -pinene oxidation by O<sub>3</sub> is likely to be minor at night in all but the most pristine environments.  $\beta$ -Pinene dis-

plays a rather extreme manifestation of this observation, but all four monoterpenes studied have NO<sub>2</sub> / BVOC ratios such that NO<sub>3</sub> oxidation is likely to dominate even in relatively remote regions.

The complexity shown by just these four BVOCs reacting with two different oxidants suggests that bulk parameters in global and regional models need to be very carefully considered if they are going to accurately match observed ambient organic aerosol loadings. These models use one or two, typically daytime, aerosol yield parameters for bulk monoterpenes – often considering  $\alpha$ -pinene or  $\beta$ -pinene yields to be representative (e.g., Lane et al., 2008). To the knowledge of the authors, the modeling approaches of Hoyle et al. (2007) and Pye et al. (2010) are the only global-scale models that parameterize NO<sub>3</sub> chemistry. Future challenges in constraining the global aerosol budget will likely require creating more nuanced approaches to modeling different regions with ostensibly similar chemistry that has been shown to have diverse effects on aerosol formation.

**The Supplement related to this article is available online at doi:10.5194/acp-15-12267-2015-supplement.**

*Acknowledgements.* J. L. Fry and D. C. Draper gratefully acknowledge funding from the National Center for Environmental Research (NCER) STAR Program, EPA no. RD-83539901, as well as the Reed College Class of '21 Award. We thank Rhiana Meade for the development of the RECv1.0 as well as Dean Atkinson for his donation of PFA film to build the RECv2.0 used in this study. D. K. Farmer acknowledges the National Science Foundation (AGS 1240611) for its support.

Edited by: A. Virtanen

## References

- Atkinson, R. and Arey, J.: Atmospheric Degradation of Volatile Organic Compounds, *Chem. Rev.*, 103, 4605–4638, doi:10.1021/cr0206420, 2003.
- Atkinson, R., Aschmann, S. M., Arey, J., and Shorees, B.: Formation of OH radicals in the gas phase reactions of O<sub>3</sub> with a series of terpenes, *J. Geophys. Res.-Atmos.*, 97, 6065–6073, doi:10.1029/92JD00062, 1992.
- Ayres, B. R., Allen, H. M., Draper, D. C., Brown, S. S., Wild, R. J., Jimenez, J. L., Day, D. A., Campuzano-Jost, P., Hu, W., de Gouw, J., Koss, A., Cohen, R. C., Duffey, K. C., Romer, P., Baumann, K., Edgerton, E., Takahama, S., Thornton, J. A., Lee, B. H., Lopez-Hilfiker, F. D., Mohr, C., Goldstein, A. H., Olson, K., and Fry, J. L.: Organic nitrate aerosol formation via NO<sub>3</sub> + BVOC in the Southeastern US, *Atmos. Chem. Phys. Discuss.*, 15, 16235–16272, doi:10.5194/acpd-15-16235-2015, 2015.
- Barthelme, R. J. and Pryor, S. C.: A model mechanism to describe oxidation of monoterpenes leading to secondary organic aerosol: 1.  $\alpha$ -pinene and  $\beta$ -pinene, *J. Geophys. Res.-Atmos.*, 104, 23657–23699, doi:10.1029/1999JD900382, 1999.
- Bateman, A. P., Walser, M. L., Desyaterik, Y., Laskin, J., Laskin, A., and Nizkorodov, S. A.: The Effect of Solvent on the Analysis of Secondary Organic Aerosol Using Electrospray Ionization Mass Spectrometry, *Environ. Sci. Technol.*, 42, 7341–7346, doi:10.1021/es801226w, 2008.
- Bateman, A. P., Laskin, J., Laskin, A., and Nizkorodov, S. A.: Applications of High-Resolution Electrospray Ionization Mass Spectrometry to Measurements of Average Oxygen to Carbon Ratios in Secondary Organic Aerosols, *Environ. Sci. Technol.*, 46, 8315–8324, doi:10.1021/es3017254, 2012.
- Boyd, C. M., Sanchez, J., Xu, L., Eugene, A. J., Nah, T., Tuet, W. Y., Guzman, M. I., and Ng, N. L.: Secondary organic aerosol formation from the  $\beta$ -pinene+NO<sub>3</sub> system: effect of humidity and peroxy radical fate, *Atmos. Chem. Phys.*, 15, 7497–7522, doi:10.5194/acp-15-7497-2015, 2015.
- Carlton, A. G., Pinder, R. W., Bhave, P. V., and Pouliot, G. A.: To What Extent Can Biogenic SOA be Controlled?, *Environ. Sci. Technol.*, 44, 3376–3380, doi:10.1021/es903506b, 2010.
- Crounse, J. D., Nielsen, L. B., Jørgensen, S., Kjaergaard, H. G., and Wennberg, P. O.: Autoxidation of Organic Compounds in the Atmosphere, *J. Phys. Chem. Lett.*, 4, 3513–3520, doi:10.1021/jz4019207, 2013.
- Davidson, C. I., Phalen, R. F., and Solomon, P. A.: Airborne Particulate Matter and Human Health: A Review, *Aerosol Sci. Technol.*, 39, 737–749, doi:10.1080/02786820500191348, 2005.
- Desyaterik, Y., Sun, Y., Shen, X., Lee, T., Wang, X., Wang, T., and Collett, J. L.: Speciation of “brown” carbon in cloud water impacted by agricultural biomass burning in eastern China, *J. Geophys. Res.-Atmos.*, 118, 7389–7399, doi:10.1002/jgrd.50561, 2013.
- Doezema, L. A., Longin, T., Cody, W., Perraud, V., Dawson, M. L., Ezell, M. J., Greaves, J., Johnson, K. R., and Finlayson-Pitts, B. J.: Analysis of secondary organic aerosols in air using extractive electrospray ionization mass spectrometry (EESI-MS), *RSC Adv.*, 2, 2930–2938, doi:10.1039/C2RA00961G, 2012.
- Donahue, N. M., Epstein, S. A., Pandis, S. N., and Robinson, A. L.: A two-dimensional volatility basis set: 1. organic-aerosol mixing thermodynamics, *Atmos. Chem. Phys.*, 11, 3303–3318, doi:10.5194/acp-11-3303-2011, 2011.
- Ehn, M., Thornton, J. A., Kleist, E., Sipila, M., Junninen, H., Pullinen, I., Springer, M., Rubach, F., Tillmann, R., Lee, B., Lopez-Hilfiker, F., Andres, S., Acir, I.-H., Rissanen, M., Jokinen, T., Schobesberger, S., Kangasluoma, J., Kontkanen, J., Nieminen, T., Kurten, T., Nielsen, L. B., Jørgensen, S., Kjaergaard, H. G., Canagaratna, M., Maso, M. D., Berndt, T., Petaja, T., Wahner, A., Kerminen, V.-M., Kulmala, M., Worsnop, D. R., Wildt, J., and Mentel, T. F.: A large source of low-volatility secondary organic aerosol, *Nature*, 506, 476–479, doi:10.1038/nature13032, 2014.
- Fry, J. L., Kiendler-Scharr, A., Rollins, A. W., Wooldridge, P. J., Brown, S. S., Fuchs, H., Dubé, W., Mensah, A., dal Maso, M., Tillmann, R., Dorn, H.-P., Brauers, T., and Cohen, R. C.: Organic nitrate and secondary organic aerosol yield from NO<sub>3</sub> oxidation of  $\beta$ -pinene evaluated using a gas-phase kinetics/aerosol partitioning model, *Atmos. Chem. Phys.*, 9, 1431–1449, doi:10.5194/acp-9-1431-2009, 2009.

- Fry, J. L., Kiendler-Scharr, A., Rollins, A. W., Brauers, T., Brown, S. S., Dorn, H.-P., Dubé, W. P., Fuchs, H., Mensah, A., Rohrer, F., Tillmann, R., Wahner, A., Wooldridge, P. J., and Cohen, R. C.: SOA from limonene: role of NO<sub>3</sub> in its generation and degradation, *Atmos. Chem. Phys.*, 11, 3879–3894, doi:10.5194/acp-11-3879-2011, 2011.
- Fry, J. L., Draper, D. C., Zarzana, K. J., Campuzano-Jost, P., Day, D. A., Jimenez, J. L., Brown, S. S., Cohen, R. C., Kaser, L., Hansel, A., Cappellin, L., Karl, T., Hodzic Roux, A., Turnipseed, A., Cantrell, C., Lefer, B. L., and Grossberg, N.: Observations of gas- and aerosol-phase organic nitrates at BEACHON-RoMBAS 2011, *Atmos. Chem. Phys.*, 13, 8585–8605, doi:10.5194/acp-13-8585-2013, 2013.
- Fry, J. L., Draper, D. C., Barsanti, K. C., Smith, J. N., Ortega, J., Winkler, P. M., Lawler, M. J., Brown, S. S., Edwards, P. M., Cohen, R. C., and Lee, L.: Secondary Organic Aerosol Formation and Organic Nitrate Yield from NO<sub>3</sub> Oxidation of Biogenic Hydrocarbons, *Environ. Sci. Technol.*, 48, 11944–11953, doi:10.1021/es502204x, 2014.
- Fry, J. L., Koski, C., Bott, K., Hsu-Flanders, R., and Hazell, M.: Downwind particulate matters: Regulatory implications of secondary aerosol formation from the interaction of nitrogen oxides and tree emissions, *Environ. Sci. Policy*, 50, 180–190, doi:10.1016/j.envsci.2015.02.017, 2015.
- Geron, C., Rasmussen, R., Arnsts, R. R., and Guenther, A.: A review and synthesis of monoterpene speciation from forests in the United States, *Atmos. Environ.*, 34, 1761–1781, doi:10.1016/S1352-2310(99)00364-7, 2000.
- Glasius, M., Lahaniati, M., Calogirou, A., Di Bella, D., Jensen, N. R., Hjorth, J., Kotzias, D., and Larsen, B. R.: Carboxylic Acids in Secondary Aerosols from Oxidation of Cyclic Monoterpenes by Ozone, *Environ. Sci. Technol.*, 34, 1001–1010, doi:10.1021/es990445r, 2000.
- Goldstein, A. H. and Galbally, I. E.: Known and Unexplored Organic Constituents in the Earth's Atmosphere, *Environ. Sci. Technol.*, 41, 1514–1521, doi:10.1021/es072476p, 2007.
- Griffin, R. J., Cocker, D. R., Flagan, R. C., and Seinfeld, J. H.: Organic aerosol formation from the oxidation of biogenic hydrocarbons, *J. Geophys. Res.-Atmos.*, 104, 3555–3567, doi:10.1029/1998JD100049, 1999.
- Grosjean, D. and Harrison, J.: Response of chemiluminescence NO<sub>x</sub> analyzers and ultraviolet ozone analyzers to organic air pollutants, *Environ. Sci. Technol.*, 19, 862–865, doi:10.1021/es00139a016, 1985.
- Guenther, A., Hewitt, C. N., Erickson, D., Fall, R., Geron, C., Graedel, T., Harley, P., Klinger, L., Lerdau, M., McKay, W. A., Pierce, T., Scholes, B., Steinbrecher, R., Tallamraju, R., Taylor, J., and Zimmerman, P.: A global model of natural volatile organic compound emissions, *J. Geophys. Res.-Atmos.*, 100, 8873–8892, doi:10.1029/94JD02950, 1995.
- Hallquist, M., Wängberg, I., Ljungström, E., Barnes, I., and Becker, K.-H.: Aerosol and Product Yields from NO<sub>3</sub> Radical-Initiated Oxidation of Selected Monoterpenes, *Environ. Sci. Technol.*, 33, 553–559, doi:10.1021/es980292s, 1999.
- Hallquist, M., Wenger, J. C., Baltensperger, U., Rudich, Y., Simpson, D., Claeys, M., Dommen, J., Donahue, N. M., George, C., Goldstein, A. H., Hamilton, J. F., Herrmann, H., Hoffmann, T., Iinuma, Y., Jang, M., Jenkin, M. E., Jimenez, J. L., Kiendler-Scharr, A., Maenhaut, W., McFiggans, G., Mentel, Th. F., Monod, A., Prévôt, A. S. H., Seinfeld, J. H., Surratt, J. D., Szmigielski, R., and Wildt, J.: The formation, properties and impact of secondary organic aerosol: current and emerging issues, *Atmos. Chem. Phys.*, 9, 5155–5236, doi:10.5194/acp-9-5155-2009, 2009.
- Haynes, W., Bruno, T. J., and Lide, D. R. (Eds.): *CRC Handbook of Chemistry and Physics*, 93rd Edn. (Internet Version), CRC Press/Taylor and Francis, 2012.
- Heald, C. L., Jacob, D. J., Park, R. J., Russell, L. M., Huebert, B. J., Seinfeld, J. H., Liao, H., and Weber, R. J.: A large organic aerosol source in the free troposphere missing from current models, *Geophys. Res. Lett.*, 32, L18809, doi:10.1029/2005GL023831, 2005.
- Heald, C. L., Coe, H., Jimenez, J. L., Weber, R. J., Bahreini, R., Middlebrook, A. M., Russell, L. M., Jolleys, M., Fu, T.-M., Allan, J. D., Bower, K. N., Capes, G., Crosier, J., Morgan, W. T., Robinson, N. H., Williams, P. I., Cubison, M. J., DeCarlo, P. F., and Dunlea, E. J.: Exploring the vertical profile of atmospheric organic aerosol: comparing 17 aircraft field campaigns with a global model, *Atmos. Chem. Phys.*, 11, 12673–12696, doi:10.5194/acp-11-12673-2011, 2011.
- Hoffmann, T., Odum, J., Bowman, F., Collins, D., Klockow, D., Flagan, R., and Seinfeld, J.: Formation of organic aerosols from the oxidation of biogenic hydrocarbons, *J. Atmos. Chem.*, 26, 189–222, 1997.
- Hoyle, C. R., Berntsen, T., Myhre, G., and Isaksen, I. S. A.: Secondary organic aerosol in the global aerosol – chemical transport model Oslo CTM2, *Atmos. Chem. Phys.*, 7, 5675–5694, doi:10.5194/acp-7-5675-2007, 2007.
- Hoyle, C. R., Boy, M., Donahue, N. M., Fry, J. L., Glasius, M., Guenther, A., Hallar, A. G., Huff Hartz, K., Petters, M. D., Petäjä, T., Rosenoern, T., and Sullivan, A. P.: A review of the anthropogenic influence on biogenic secondary organic aerosol, *Atmos. Chem. Phys.*, 11, 321–343, doi:10.5194/acp-11-321-2011, 2011.
- IPCC: *Climate Change 2013: The Physical Science Basis. Contribution of Working Group I to the Fifth Assessment Report of the Intergovernmental Panel on Climate Change*, Cambridge University Press, Cambridge, United Kingdom and New York, NY, USA, doi:10.1017/CBO9781107415324, 2013.
- Jokinen, T., Sipilä, M., Richters, S., Kerminen, V.-M., Paasonen, P., Stratmann, F., Worsnop, D., Kulmala, M., Ehn, M., Herrmann, H., and Berndt, T.: Rapid Autoxidation Forms Highly Oxidized RO<sub>2</sub> Radicals in the Atmosphere, *Angew. Chem. Int. Edit.*, 53, 14596–14600, doi:10.1002/anie.201408566, 2014.
- Kroll, J. H. and Seinfeld, J. H.: Chemistry of secondary organic aerosol: Formation and evolution of low-volatility organics in the atmosphere, *Atmos. Environ.*, 42, 3593–3624, doi:10.1016/j.atmosenv.2008.01.003, 2008.
- Lane, T. E., Donahue, N. M., and Pandis, S. N.: Effect of NO<sub>x</sub> on Secondary Organic Aerosol Concentrations, *Environ. Sci. Technol.*, 42, 6022–6027, doi:10.1021/es703225a, 2008.
- Lee, A., Goldstein, A. H., Kroll, J. H., Ng, N. L., Varutbangkul, V., Flagan, R. C., and Seinfeld, J. H.: Gas-phase products and secondary aerosol yields from the photooxidation of 16 different terpenes, *J. Geophys. Res.-Atmos.*, 111, D17305, doi:10.1029/2006JD007050, 2006.
- McMurry, P. H. and Grosjean, D.: Gas and aerosol wall losses in Teflon film smog chambers, *Environ. Sci. Technol.*, 19, 1176–1182, doi:10.1021/es00142a006, 1985.

- Middleton, P.: Sources of air pollutants, in: Composition, Chemistry, and Climate of the Atmosphere, edited by: Singh, H. B., Van Nostrand Reinhold, New York, 1995.
- Moldanova, J. and Ljungström, E.: Modelling of particle formation from NO<sub>3</sub> oxidation of selected monoterpenes, *J. Aerosol Sci.*, 21, 1317–1333, doi:10.1016/S0021-8502(00)00041-0, 2000.
- Ng, N. L., Kroll, J. H., Keywood, M. D., Bahreini, R., Varutbangkul, V., Flagan, R. C., Seinfeld, J. H., Lee, A., and Goldstein, A. H.: Contribution of First- versus Second-Generation Products to Secondary Organic Aerosols Formed in the Oxidation of Biogenic Hydrocarbons, *Environ. Sci. Technol.*, 40, 2283–2297, doi:10.1021/es052269u, 2006.
- Perraud, V., Bruns, E. A., Ezell, M. J., Johnson, S. N., Greaves, J., and Finlayson-Pitts, B. J.: Identification of Organic Nitrates in the NO<sub>3</sub> Radical Initiated Oxidation of  $\alpha$ -Pinene by Atmospheric Pressure Chemical Ionization Mass Spectrometry, *Environ. Sci. Technol.*, 44, 5887–5893, doi:10.1021/es1005658, 2010.
- Perraud, V., Bruns, E. A., Ezell, M. J., Johnson, S. N., Yu, Y., Alexander, M. L., Zelenyuk, A., Imre, D., Chang, W. L., Dabdub, D., Pankow, J. F., and Finlayson-Pitts, B. J.: Nonequilibrium atmospheric secondary organic aerosol formation and growth, *Proc. Natl. Aca. Sci.*, 109, 2836–2841, doi:10.1073/pnas.1119909109, 2012.
- Pope III, C. A., Bates, D. V., and Raizenne, M. E.: Health Effects of Particulate Air Pollution: Time for Reassessment?, *Environ. Health Perspect.*, 103, 472–480, doi:10.2307/3432586, 1995.
- Presto, A. A., Huff Hartz, K. E., and Donahue, N. M.: Secondary Organic Aerosol Production from Terpene Ozonolysis. 2. Effect of NO<sub>x</sub> Concentration, *Environ. Sci. Technol.*, 39, 7046–7054, 2005.
- Pye, H. O. T., Chan, A. W. H., Barkley, M. P., and Seinfeld, J. H.: Global modeling of organic aerosol: the importance of reactive nitrogen (NO<sub>x</sub> and NO<sub>3</sub>), *Atmos. Chem. Phys.*, 10, 11261–11276, doi:10.5194/acp-10-11261-2010, 2010.
- Reis, S., Pinder, R. W., Zhang, M., Lijie, G., and Sutton, M. A.: Reactive nitrogen in atmospheric emission inventories, *Atmos. Chem. Phys.*, 9, 7657–7677, doi:10.5194/acp-9-7657-2009, 2009.
- Rollins, A. W., Browne, E. C., Min, K.-E., Pusede, S. E., Wooldridge, P. J., Gentner, D. R., Goldstein, A. H., Liu, S., Day, D. A., Russell, L. M., and Cohen, R. C.: Evidence for NO<sub>x</sub> Control over Nighttime SOA Formation, *Science*, 337, 1210–1212, doi:10.1126/science.1221520, 2012.
- Sakulyanontvittaya, T., Duhl, T., Wiedinmyer, C., Helmig, D., Matsunaga, S., Potosnak, M., Milford, J., and Guenther, A.: Monoterpene and Sesquiterpene Emission Estimates for the United States, *Environ. Sci. Technol.*, 42, 1623–1629, doi:10.1021/es702274e, 2008.
- Sander, S., Abbatt, J., Barker, J. R., Burkholder, J. B., Friedl, R. R., Golden, D. M., Huie, R. E., Kolb, C. E., Kurylo, M. J., Moortgat, G. K., Orkin, V. L., and Wine, P. H.: Chemical Kinetics and Photochemical Data for Use in Atmospheric Studies, Evaluation Number 17, JPL Publication, 10, 1–11, 2011.
- Spittler, M., Barnes, I., Bejan, I., Brockmann, K., Benter, T., and Wirtz, K.: Reactions of NO<sub>3</sub> radicals with limonene and  $\alpha$ -pinene: Product and SOA formation, *Atmos. Environ.*, 40, 116–127, doi:10.1016/j.atmosenv.2005.09.093, 2006.
- Surratt, J. D., Murphy, S. M., Kroll, J. H., Ng, N. L., Hildebrandt, L., Sorooshian, A., Szmigielski, R., Vermeylen, R., Maenhaut, W., Claeys, M., Flagan, R. C., and Seinfeld, J. H.: Chemical Composition of Secondary Organic Aerosol Formed from the Photooxidation of Isoprene, *J. Phys. Chem. A*, 110, 9665–9690, doi:10.1021/jp061734m, 2006.
- VanReken, T. M., Greenberg, J. P., Harley, P. C., Guenther, A. B., and Smith, J. N.: Direct measurement of particle formation and growth from the oxidation of biogenic emissions, *Atmos. Chem. Phys.*, 6, 4403–4413, doi:10.5194/acp-6-4403-2006, 2006.
- Vaughan, S., Canosa-Mas, C. E., Pfrang, C., Shallcross, D. E., Watson, L., and Wayne, R. P.: Kinetic studies of reactions of the nitrate radical (NO<sub>3</sub>) with peroxy radicals (RO<sub>2</sub>): an indirect source of OH at night?, *Phys. Chem. Chem. Phys.*, 8, 3749–3760, doi:10.1039/B605569A, 2006.
- Walser, M. L., Desyaterik, Y., Laskin, J., Laskin, A., and Nizkorodov, S. A.: High-resolution mass spectrometric analysis of secondary organic aerosol produced by ozonation of limonene, *Phys. Chem. Chem. Phys.*, 10, 1009–1022, doi:10.1039/B712620D, 2008.
- Wangberg, I., Barnes, I., and Becker, K. H.: Product and Mechanistic Study of the Reaction of NO<sub>3</sub> Radicals with  $\alpha$ -Pinene, *Environ. Sci. Technol.*, 31, 2130–2135, doi:10.1021/es960958n, 1997.
- Winer, A. M., Peters, J. W., Smith, J. P., and Pitts, J. N.: Response of commercial chemiluminescent nitric oxide-nitrogen dioxide analyzers to other nitrogen-containing compounds, *Environ. Sci. Technol.*, 8, 1118–1121, doi:10.1021/es60098a004, 1974.
- Winkler, P. M., Ortega, J., Karl, T., Cappellin, L., Friedli, H. R., Barsanti, K., McMurry, P. H., and Smith, J. N.: Identification of the biogenic compounds responsible for size-dependent nanoparticle growth, *Geophys. Res. Lett.*, 39, L20815, doi:10.1029/2012GL053253, 2012.
- Xu, L., Guo, H., Boyd, C. M., Klein, M., Bougiatioti, A., Cerully, K. M., Hite, J. R., Isaacman-VanWertz, G., Kreisberg, N. M., Knote, C., Olson, K., Koss, A., Goldstein, A. H., Hering, S. V., de Gouw, J., Baumann, K., Lee, S.-H., Nenes, A., Weber, R. J., and Ng, N. L.: Effects of anthropogenic emissions on aerosol formation from isoprene and monoterpenes in the southeastern United States, *Proc. Natl. Acad. Sci.*, 112, 37–42, doi:10.1073/pnas.1417609112, 2015.
- Yu, J., Cocker, D., Griffin, R., Flagan, R., and Seinfeld, J.: Gas-phase ozone oxidation of monoterpenes: Gaseous and particulate products, *J. Atmos. Chem.*, 34, 207–258, 1999.
- Zhang, X., Cappa, C. D., Jathar, S. H., McVay, R. C., Ensberg, J. J., Kleeman, M. J., and Seinfeld, J. H.: Influence of vapor wall loss in laboratory chambers on yields of secondary organic aerosol, *Proc. Natl. Aca. Sci.*, 111, 5802–5807, 2014.
- Zhao, J., Ortega, J., Chen, M., McMurry, P. H., and Smith, J. N.: Dependence of particle nucleation and growth on high-molecular-weight gas-phase products during ozonolysis of  $\alpha$ -pinene, *Atmos. Chem. Phys.*, 13, 7631–7644, doi:10.5194/acp-13-7631-2013, 2013.